Science Case for ALMA Band 5

edited by Robert Laing (ESO)

Christian Brinch (Leiden), Jose Cernicharo (CSIC-INTA, Madrid), Elizabeth Humphreys (ESO), Jes Joergensen (Centre for Star and Planet Formation, Copenhagen), Mark Lacy (NRAO), Roberto Maiolino (INAF-OAR), Raphael Moreno (Observatoire de Paris), Anita Richards (JBCA, Manchester), Leonardo Testi (ESO), Fabian Walter (MPIA, Heidelberg).

Executive Summary

We present a set of scientific projects which together make up a compelling case for equipping ALMA with a full set of Band 5 (163 - 211 GHz) receivers. There are two key areas: (i) detecting and studying the dynamics of the first galaxies through their [CII] emission and (ii) imaging water vapour in the Solar System and in regions of planet formation. We also outline a broad range of other science cases. We stress that ALMA Band 5 will be a unique capability and an essential complement to future ground-based and space observatories.

1 Introduction

When ALMA was originally conceived, it was planned to equip it with receivers covering all of the atmospheric transmission windows between 30 and 950 GHz. In order to reduce costs, however, it will be equipped initially with a subset of the receiver bands that are finally envisaged. The initial receiver bands selected were those deemed to be both feasible and of the highest scientific interest when construction was approved. ALMA Band 5 (163 – 211 GHz), although always considered to be scientifically important, was placed at lower priority, primarily because of the difficulty of observing close to the strong atmospheric water line at 183 GHz. Following the accumulation of statistics showing that the transparency of the Chajnantor site around the water line is better than expected and the development of improved phase-correction techniques, a proposal to support the construction of six Band 5 receivers for ALMA was supported by the European Commission (EC) under the Framework Programme 6 (FP6). The main scientific motivation was the synergy between ALMA Band 5 and the HIFI instrument on the Herschel satellite, which is currently in full operation. ALMA Band 5 will allow us to resolve and image emission from water and its isotopes, which are being detected by Herschel at other (typically shorter) wavelengths invisible from the ground. The small complement of Band 5 receivers will be installed at the ALMA Observatory by 2013.

Since the initial proposal to the EC, the scientific case for Band 5 has strengthened and initial tests of the first receivers demonstrate that they meet the ALMA specifications. In this document, we re-evaluate the scientific potential and goals of an ALMA fully equipped with Band 5. Over the last decade, and especially in the last few years, there has been an increasing interest in observations at the frequencies offered by the ALMA Band 5, for both Galactic and extragalactic science. Water is, of course, of intense interest because of its role in the origin of life. A key application for Band 5 is therefore high-resolution imaging of the water line at 183 GHz in our own Solar System, Galactic and nearby extragalactic sources. In addition, the $158\mu m$ line of ionized carbon from objects at redshifts between 8.0 and 10.65 will appear in the band, opening up the possibility of probing the earliest epoch of galaxy formation.

In Sections 2 and 3, we discuss the two key science areas for Band 5: [CII] emission from the earliest galaxies and water in star formation and the Solar System. A wide variety of other interesting science projects will be possible with a full set of Band 5 receivers: several are outlined in Section 4. We summarise our conclusions in Section 5. A few important performance numbers are given in Appendix A.

2 Key Science Topic 1: The Earliest Galaxies

A key frontier in the exploration of the Universe is the Epoch of Reionization (EoR), during which the first galaxies formed. We now know from observations of the Cosmic Microwave Background and the Gunn-

Peterson effect in quasar spectra that the EoR spans the redshift range $6 < z < 15$. Key questions about this period include:

- What are the ionizing sources?

- What are the gas masses of the first galaxies, i.e. how much fuel is available for star formation?

- How and in what numbers are stars formed?

- What are the dynamical masses?

Finding objects in the redshift range $6 < z < 10$ is now becoming possible with a variety of techniques: quasar surveys [28], near-IR dropouts [3, 4], searches for Lyman α emission and gamma-ray burst follow-up [34], for example. Studying the gas content of these systems is a very active sub-field of mm-wave astronomy.

Imaging of high-redshift quasars in various CO transitions has been particularly successful, but studying the gas in other types of high-redshift galaxy is more problematic. In quasars, many of the high-J CO transitions are excited and can be detected in multiple ALMA bands. In more 'normal' (sub-mm selected or BzK dropout) galaxies, only the lowest CO transitions are expected to be excited and even these may be very weak.

An alternative tracer of the interstellar medium is one of the main cooling lines, the fine-structure [CII] line at 158μm. This is expected to be much stronger than the CO lines and space-based observations have indeed demonstrated that this single line can carry a large fraction of the total FIR luminosity of an entire galaxy, with $L_{\rm CII}/L_{\rm FIR} \approx 0.01$ in some cases. This line is observable in ALMA Band 5 for $8.0 < z < 10.65$ and has already been detected and imaged in a quasar at $z = 6.4$ [23, 37] (Fig 1).

A number of lines of evidence suggest that [CII] will be by some way the strongest line in the highest-redshift sub-mm galaxies.

1. The ratio $L_{\rm CII}/L_{\rm FIR}$ tends to decrease with $L_{\rm FIR}$, with significantly smaller values observed in the most intrinsically luminous objects, particularly AGN (Fig. 2, left panel; [33]).

2. As mentioned earlier, the higher-order CO transitions are unlikely to be excited. Fig. 2 (right panel) shows the range of CO transitions which are expected from various different types of object in the ALMA and EVLA bands as functions of redshift.

3. Low-order CO transitions also appear to be weak compared with [CII]. For example, $L_{\rm CII}/L_{\rm [CO1-0]} \approx 10^4$ in a sub-mm galaxy at $z = 4.7$ [6].

4. The first galaxies are expected to have low metallicity. At first sight this would tend to suggest that [CII] emission would be weaker, but Herschel observations show that the nearby dwarf galaxy NGC 4214 (which has 1/3 solar metallicity) has $L_{\rm [CII]}/L_{\rm FIR} \approx 0.01$ and $L_{\rm [CII]}/L_{\rm CO} \approx 50000$. The Large Magellanic Could (marked on Fig. 2) also has $L_{\rm [CII]}/L_{\rm FIR} > 0.01$.

5. Absorption-line spectroscopy of high-redshift damped Lyman α systems also shows a much higher carbon abundance than predicted by naive models [30].

An estimate of the expected density of sources on the sky can be made using current constraints on the galaxy population at $z > 7$ from HAWK-I and WFC3 observations of $m_{\rm AB} \approx 28.5$ dropouts. Fig. 3 shows a rough estimate of the predicted source count in Band 5, assuming a velocity width of $150\,\rm km\,s^{-1}$ for the [CII] line. There is a low predicted density of sources, mostly in the upper part of the frequency band. A blind survey would be feasible, but several 10-hour observations would be needed.

A better observing strategy would probably be to target galaxies identified by other facilities. Candidates identified as IR dropouts are already available. In the future, the NIRspec instrument on JWST is expected to find and determine precise redshifts for roughly 10 $z > 8$ galaxies in a 4×3 arcmin^2 deep field, but will not have the spatial resolution to determine their kinematics. Alternatively, the new generation of 'redshift machines' on single dishes (ground-based, balloon-borne or in space) should provide a significant number of targets. For example, the differential Fourier-transform spectrometer proposed for the IRAM 30m telescope, which operates in the frequency range $188 - 211\,\rm GHz$ ($8 < z < 9.1$ for the [CII] line) should detect and approximately localise a few objects per field of view which ALMA will be able to image.

Detecting the [CII] emission is critical to estimating the amount of molecular gas available to fuel star formation in these early galaxies. The next step is to resolve the distribution spatially. Given the expected
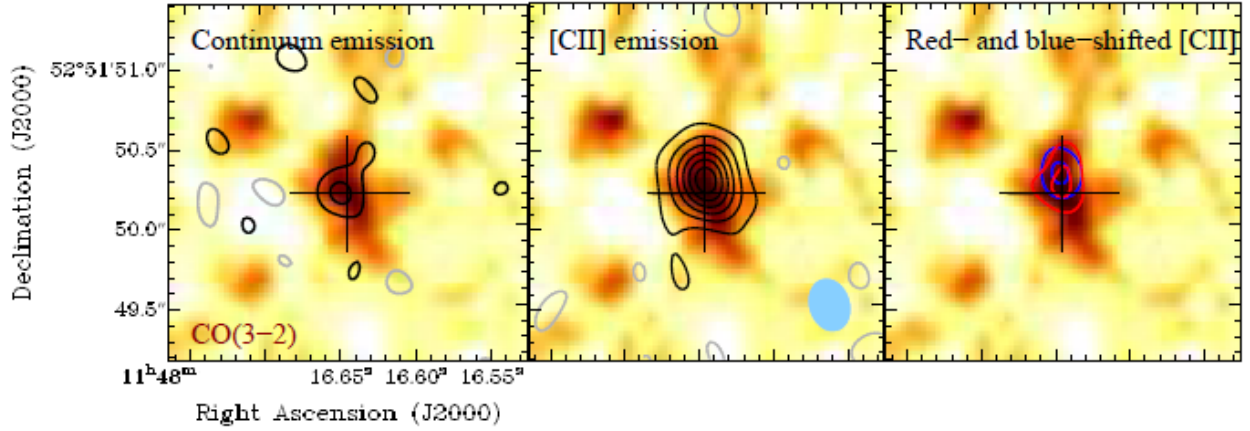
Figure 1: IRAM Plateau de Bure images of continuum and [CII] emission from a quasar at $z = 6.4$ [37]. The resolution is 0.31×0.23 arcsec^2. Left: continuum. Centre: integrated [CII]. Right: [CII] emission binned by velocity from $\pm(75 - 175)\,\mathrm{kms}^{-1}$ with respect to systemic.
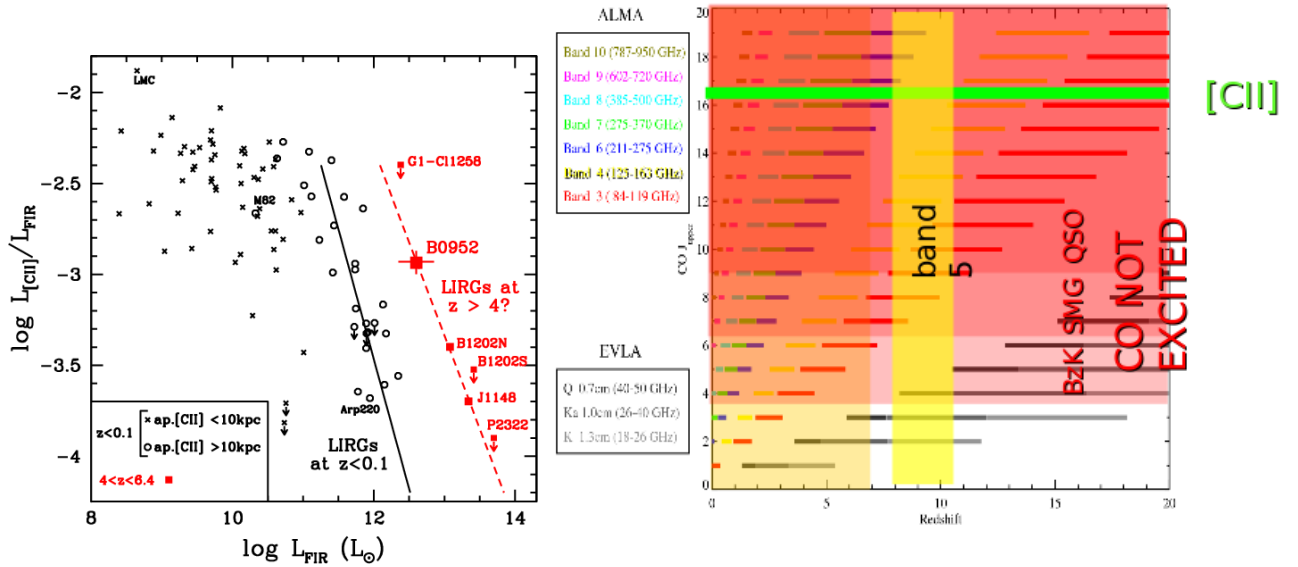

Figure 2: Left: a plot of the luminosity emitted in the [CII] line against total far-infrared luminosity, showing the tendency for the ratio $L_{\mathrm{CII}}/L_{\mathrm{FIR}}$ to reduce at high luminosity [24]. Right: the discovery space available for CO and [CII] observations with ALMA and EVLA. The horizontal lines indicate the redshifts at which CO transitions and [CII] can be observed as a function of redshift. The shaded areas correspond to CO transitions which are not expected to be excited in particular classes of object [36].
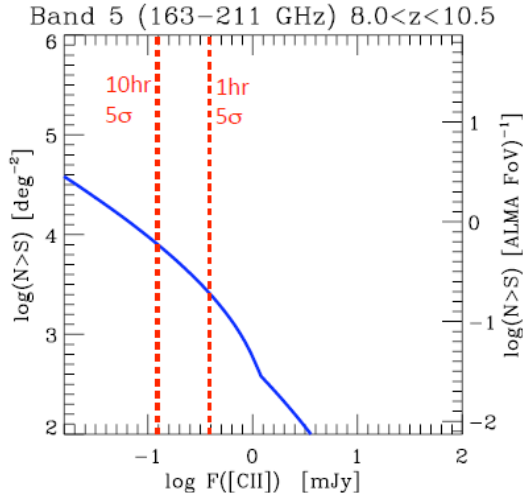
3

Figure 3: The expected source count in Band 5 for galaxies in the redshift range $8 < z < 10.5$. The plotted sensitivity limits assume 50 antennas.

diameters of many kpc, a linear resolution of $\approx$1 kpc is needed ($0.25 - 0.5$ arcsec for the redshifts in question). Such measurements are needed: (a) to estimate the size of the galaxy; (b) to measure the dynamical mass and (c) to resolve merging systems. Given the need for spectral and spatial resolution, they will require a full set of Band 5 receivers to achieve adequate sensitivity.

For observations of high-redshift [CII] the 183-GHz water line is, of course, a problem, but a manageable one. The excluded frequency range is approximately 180–186 GHz,depending on conditions. This corresponds to $9.21 < z < 9.56$. The remainder of the band is relatively unobscured.

We conclude that imaging of the first galaxies in [CII] is a unique, feasible and astrophysically important application for a full set of Band 5 receivers on ALMA.

3 Key Science Topic 2: Water in Planetary and Protoplanetary Systems

Water is clearly one of the most important molecules in the Solar System and beyond because of its importance for life. The creation of water from oxygen and hydrogen and the complex processes of its evolution in stars and planets (the 'water cycle') is of obvious interest (see [2] for a recent review). Water in the Earth's atmosphere prevents easy observations from the ground except for a few rare masing transitions (e.g. as discussed elsewhere in the present science case). In this section, we concentrate on the ability of ALMA to observe thermally excited emission from water vapour in the 183 GHz $3_{13} - 2_{20}$ transition of para-H_2O in protoplanetary disks and the Solar System.

3.1 Water in Protoplanetary Disks

The presence of water on Earth is obviously a key issue in the origin and development of Life. This in turn raises the question of the presence and abundance of water in protoplanetary disks, from which planets such as our own formed.

A major surprise from Herschel observations was the relative scarcity of water vapour in nearby protoplanetary disks. For example, HIFI observations of the $1_{10} - 1_{01}$ transition in DM Tau [1] only gave a tentative detection. Secure measurements in both spin isomers of water were however obtained by [16] in the closest protoplanetary disk, TW Hya, albeit at a lower level than expected.

Detailed modelling of the DM Tau disk using the LIME radiative transfer code [5] by Brinch (in preparation) initially predicted much stronger water emission than is actually detected (by a factor of about 100). A possible hypothesis to explain this is that icy grains coagulate and settle into the mid-plane of the circumstellar disk, where they are not illuminated by UV radiation from the star. Even if upward mixing of
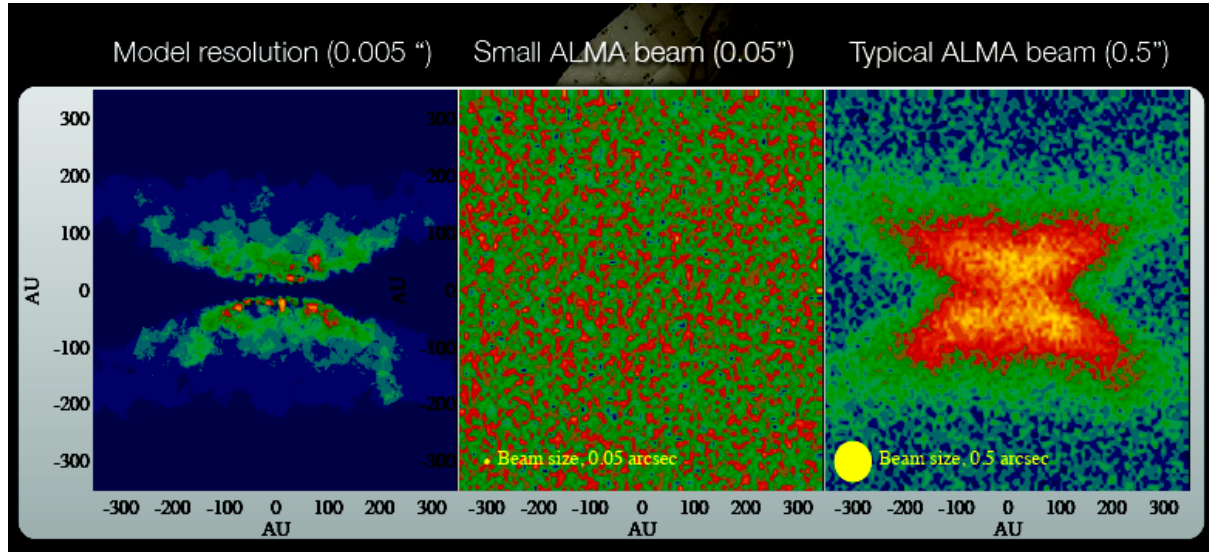
Figure 4: Simulations of ALMA Band 5 observations of the DM Tau protoplanetary disk by C. Brinch, assuming a water abundance scaled to match the observations of [1]. Left: model; centre: simulated ALMA image with noise at 0.05 arcsec resolution; right: ALMA image with noise at 0.5 arcsec resolution. The simulations assume 50 antennas

the grains occurs, large icy grains may stay put in the mid-plane. Fig.4 shows simulated observations with water abundance scaled to match the tentative HIFI line detection. The water in the disk can be imaged, but only with the full set of antennas.

There are several hundred known protoplanetary disks observable by ALMA at similar distances to DW Tau (120 – 160 pc). A detection survey in the most compact configuration would allow correlation of water-vapour emission with age, type of central star, settling properties and grain characteristics. The brightest examples could then be selected for imaging.

3.2 Planetary atmospheres

Spectrally and spatially resolved measurements of molecular lines in planetary atmospheres allow:

1. Chemical sounding, to give the distribution of species as a function of height in the atmosphere.

2. Thermal sounding to give the temperature profile.

3. Dynamical sounding (wind velocity as a function of height from the Doppler line widths).

All of these quantities are closely coupled, and three-dimensional mapping over the course of a planetary year constrains the atmospheric cycles and hence the origin and evolution of planets.

It should be possible to image Mars and Venus with good temporal and spatial resolution and also, with more effort, to study Saturn. The outer giant planets and the moons of Jupiter and Saturn will probably be too faint to image in a reasonable time.

3.2.1 The Martian water cycle

The vertically-integrated column of water on Mars is strongly variable both with latitude and season, reflecting interchange with the polar caps.The vertical profile is poorly characterised, but also appears to show seasonal variations. In particular, the hygropause appears to vary with time and there are more local changes associated with dust storms [14]. The 183-GHz water line has been detected using the IRAM 30m Telescope [11], but not spatially resolved. Fig. 5 shows the predicted spectrum from Mars. The expected signal-to-noise ratio is 40 in 1 hour for a 1 arcsec beam, so detailed, seasonally-resolved mapping should be straightforward (Mars has an average angular diameter of 14 arcsec).
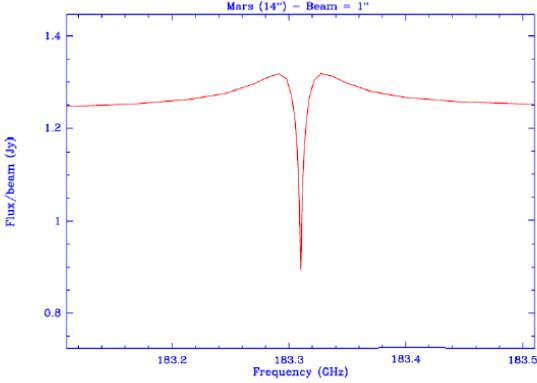
Figure 5: The predicted spectrum of Mars in the 183-GHz water line, observed with ALMA at a resolution of 1 arcsec.

In combination with observations of HDO at 225 GHz in Band 6, it would also be possible to study the Martian deuterium cycle.

3.2.2 Water on Venus

Observations of Venus at mm and sub-mm wavelengths probe mesospheric water, at heights between 60 and 100 km (i.e. above the cloud tops). The emission is highly variable [15] on short timescales as well as with planetary year. As for Mars, the 183-GHz water line has been detected, and it should be possible to image the planet with good resolution (s/n $\sim$ 40 in a 2 arcsec beam, compared with a diameter of 20 arcsec) in both this line and HDO.

3.2.3 Water on Giant Planets

Much less is known about water on the giant planets, although there have been detections with Herschel and ISO. The aim would again be to study seasonal variability, with the goal of understanding the origin of water (interplanetary dust particle flux, local sources such as rings and satellites or cometary collisions). Mapping of Saturn (20 arcsec diameter; 2 arcsec beam) with s/n $\sim$ 10 should be possible in 10 hours. Jupiter presents a technical challenge, since the predicted s/n is lower, its diameter is significantly larger than the primary beam and mosaicing would be required.

3.3 Comets

Comets are particularly important as relics of the primitive solar nebula and studies of their composition address both their origin and the chemical processes at work in the early Solar System. Emission from H_2O, $H_2^{18}O$ and H_2S has been detected from comets in space-based observations [17], but barely resolved spatially (see Fig. 6).

The role of ALMA Band 5 would be to provide high-resolution (1 arcsec, corresponding to 1000 km at a distance of 1 AU) imaging of water in comets.This would enable the study of gas sources at the surface of the cometary nucleus and in the more extended emission, and would shed light on the excitation conditions. Estimates by D. Bockelee-Morvan suggest that emission from H_2O in the 183 GHz line would be detected by ALMA with high signal-to-noise ratio with a beam of 1 arcsec in 1 hour of observation and that $H_2^{18}O$ could be imaged if the water density is high.
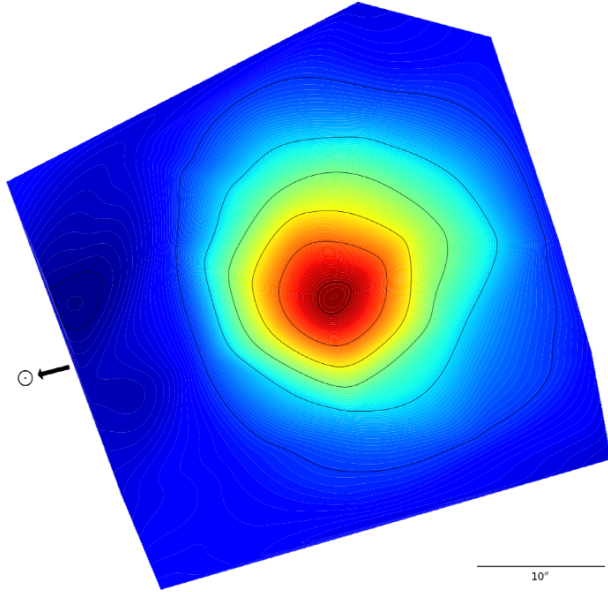
Figure 6: Map of the 2_{21}–2_{12} water line at 1661 GHz observed with PACS on Herschel in comet 103P/Hartley 2 [26].

4 A broad range of science cases

4.1 Highly redshifted atomic transitions

In addition to the [CII] line discussed in detail in Section 2, lines from other atomic transitions will be redshifted into ALMA Band 5. The most important of these is the [NII] line at a rest wavelength of 205 μm, which is in Band 5 for $5.9 < z < 8.0$. This provides information about the HII and PDR phases of the interstellar medium. Its ratio with the strength of the transition at 122 μm (in Band 7 for these redshifts) can be used as a density indicator [31].

4.2 Maser disks in external galaxies

Since the imaging of the 22-GHz water maser disk in the nearby active galaxy NGC 4258 [27], the potential of high spatial and spectral resolution observations of extragalactic maser disks has been widely recognised. There are three primary applications:

1. mapping the AGN accretion disk (warps, spiral structure);

2. accurately determining the mass of the central black hole and

3. measuring geometric distances in order to derive an accurate and unbiased value of the Hubble Constant.

(see [25] for a recent update).

Observations of 183 and 22-GHz maser emission are complementary in studying accretion disks. Models indicate that the 183-GHz maser emission is pumped:

1. at T = $400 - 1000$ K, $n_{H_2} = 10^8 - 10^{10}$ cm^{-3} and

2. at T ≈ 200 K, $n_{H_2} = 10^5 - 10^7$ cm^{-3}.

For this reason, 183-GHz maser emission is likely to originate not only from the same regions as the 22-GHz masers (in which case a comparison can be used to map out temperature and density), but also from farther out in the accretion disk. Emission may also be visible from the "back" of the disk since the relativistic plasma from the jet core is optically thin at 183 GHz but not at 22 GHz (Fig. 7; left panel).
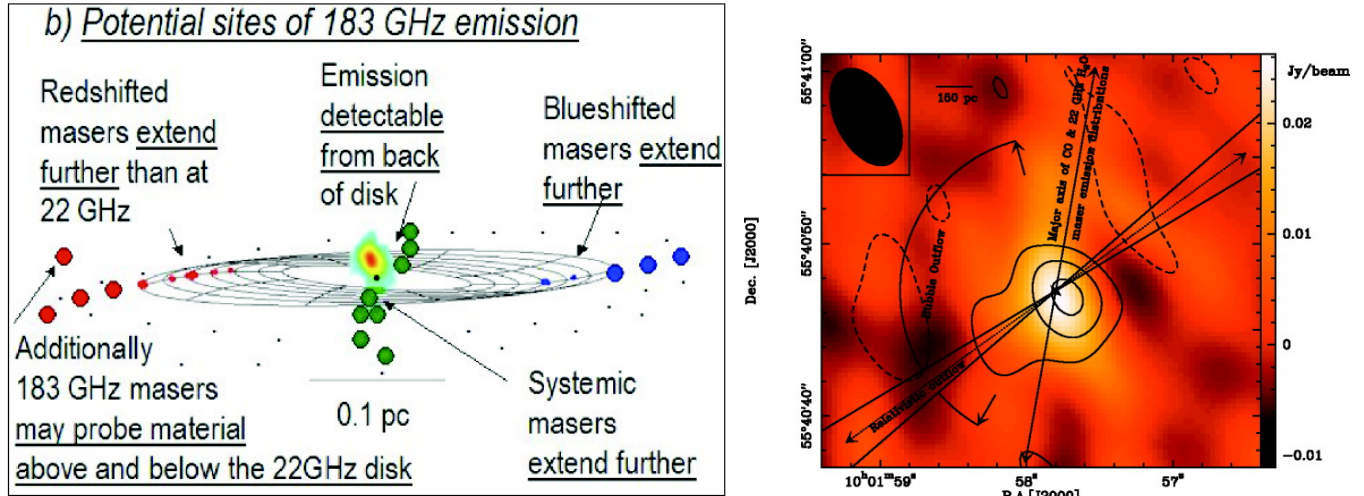
Figure 7: Left: Potential sites of 183-GHz maser emission in AGN accretion disks. Right: SMA image of 183-GHz water maser emission from the nearby galaxy NGC 3079 [20]. Contours of maser emission are superimposed on a colour representation of total intensity at 193 GHz.

More than 100 galaxies with 22-GHz maser emission are known. In contrast, no comprehensive search has been made at 183 GHz and the possibility of "supermaser disks" visible to larger distances remains open.[1] Water maser emission in the 183 GHz line associated with an AGN has so far been detected and imaged with the SMA only in the LINER galaxy NGC 3079 [20] (Fig. 7; right panel).[2]

The next step would be to survey nearby candidate galaxies, initially those with 22-GHz masers, with ALMA in a compact configuration. A source as strong as NGC 3079 at 50 Mpc (56 mJy) could be detected at 5σ in $0.5\,\mathrm{km\,s^{-1}}$ channels in 10 min for 0.5 mm PWV or at 20σ in 2.3 hr, assuming 50 antennas (the times for 6 antennas are prohibitive: 13 and 184 hr, respectively). A 20σ detection would allow astrometry at the level of 0.6 mas in the extended ALMA configurations (25 mas beam), with the important proviso that good imaging is required.

Although ALMA even in its most extended configuration is not competitive in resolution with 22-GHz global VLBI, it should certainly be possible to constrain physical conditions in the accretion disks and perhaps also to estimate black-hole masses and geometric distances.

4.3 Water maser emission from Starburst Galaxies

Bright 183-GHz water maser emission has also been detected from the starburst galaxy Arp 220 [9] using the IRAM 30 m Telescope (Fig. 8). In contrast to NGC 3079, the line is broad and no 22-GHz maser emission is detected. The line is most plausibly produced by a starburst, triggered by the ongoing merger in this object, with $\sim 10^6$ star-forming cores similar to the Galactic condensations Sgr B2(M) and Sgr B2(N) within the central kpc.

The detection of the 183-GHz line provides an additional tool for the study of physical conditions in luminous and ultraluminous infrared galaxies. The central starburst (≈ 3 arcsec at the distance of Arp 220) can be imaged straightforwardly with ALMA in similar galaxies.

4.4 Water in star-forming regions

Water is also a key molecule in regions of star formation (Fig. 9). Its abundance in the gas phase is low in cool, quiescent regions, but increases in regions of intense heating or active shocks. As mentioned in Section 3.1, it is mostly locked on the ice mantles of grains in protoplanetary disks, predominantly in the disk midplane where it is shielded from the stellar radiation. In earlier phases of star formation it is expected that a significant fraction of the ices in the envelopes around forming stars is destroyed by either the radiation

---

[1]More distant objects are easier to observe as the maser lines are redshifted clear of the worst of the atmospheric absorption.
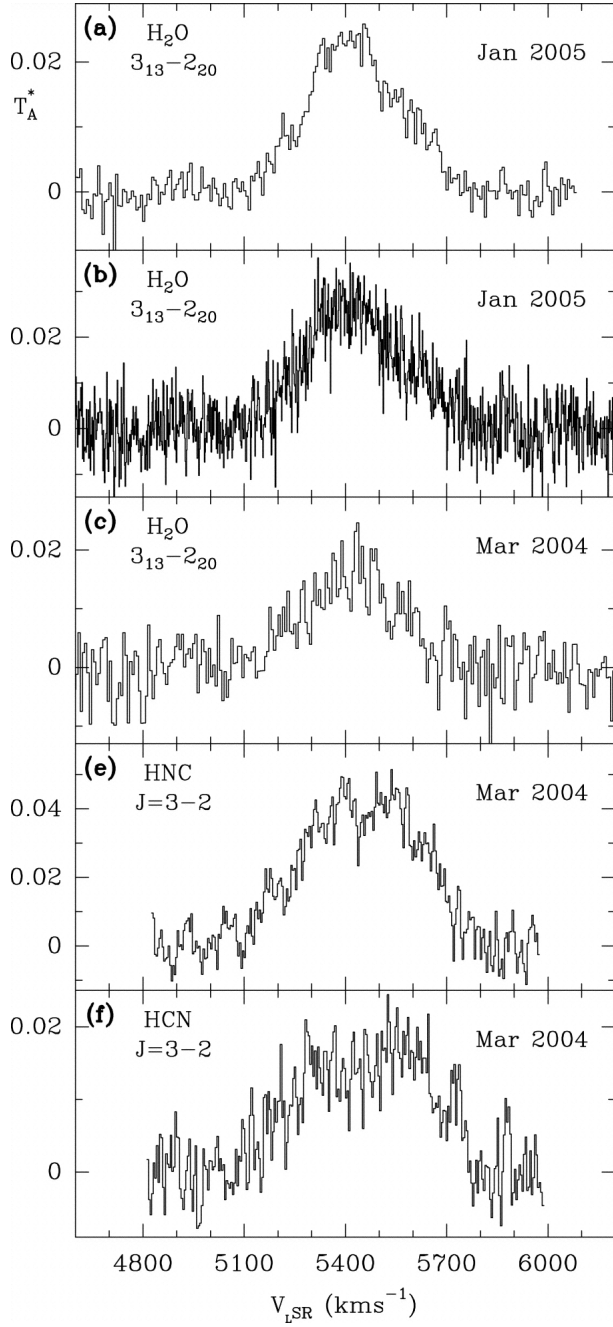[2]The very different case of Arp 220 is discussed below, Section 4.3

Figure 8: Spectra of 183-GHz water emission from the nearby starburst galaxy Arp 220 [9] compared with HCN and HNC.
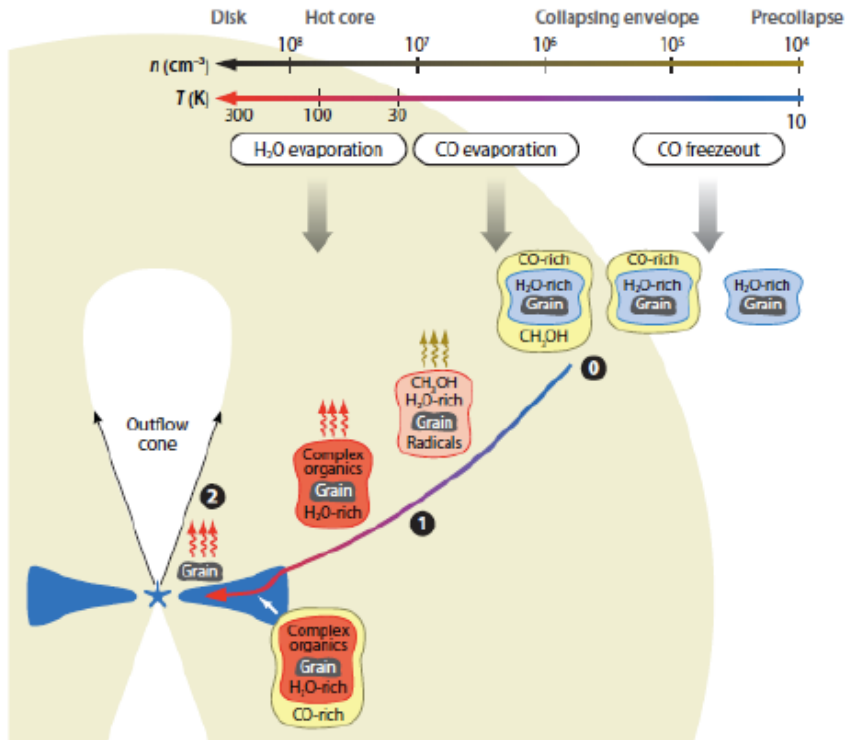
Figure 9: Schematic of low-mass star formation showing the role of water at various phases of collapse [18].

from the central forming object or by the mechanical energy deposited by protostellar outflows. Water is therefore a tracer of energetic processes in star formation; it is also the primary repository of oxygen.

Herschel observations have indeed demonstrated that water is one of the major coolants in the early phases of star formation (Karska et al., in preparation). The Herschel maps show widespread water emission tracing both the outflow and the central protostar [22, 29], with broad emission lines from warm H_2O in the protostellar outflow and narrow absorption lines from the cool envelope. An example is shown in Fig. 10. Follow-up at high angular resolution will allow us to trace the water emission and probe the physical conditions and kinematics of the emitting regions (ALMA Band 5 will be the only instrument able to resolve the emission on arcsecond scales). Given that the emission region of water, as observed by Herschel, is on relatively large scales, the ALMA observations will also have to make use of the ACA to recover the extended emission properly.

The 183-GHz line has been detected from the ground in star-forming regions using the IRAM 30 m Telescope in several low- and high-mass protostellar sources such as Orion, W49N, H7-11, and L1448-mm [7, 8]. Most lines consist of a broad component, superposed on one or more strong narrow lines. The broad component, which has been mapped in some high-mass star-forming regions such as Orion and W49N (Fig. 11), is thought to be spatially extended thermal emission, as seen in many other molecular species [7, 12]. The narrow components are likely to be maser emission. In one case, Serpens SMM1, the narrow-line emission has been imaged interferometrically using the SMA [35] and resolved into three distinct maser spots (Fig. 12). These are 500-1200 AU from the protostar, aligned in the direction of the redshifted outflow and in 2/3 cases slightly blueshifted. It is theorized that the maser spots originate in Kelvin-Helmholtz instabilities in the redshifted outflow. No extended thermal component was detected in this source. ALMA Band 5 will be able to observe these lines at higher sensitivity and resolution, possibly probing the scales at which the masers emit, and will enable the study of many more objects.

In addition to the main isotope, emission from water isotopologues, including the $H_2{}^{18}O$ $3_{1,3} - 2_{2,0}$ line (which is also in Band 5) has been detected in protostellar systems. Although extrapolation to derive the water abundance from this isopotomer is difficult, the line is much less affected by atmospheric absorption.
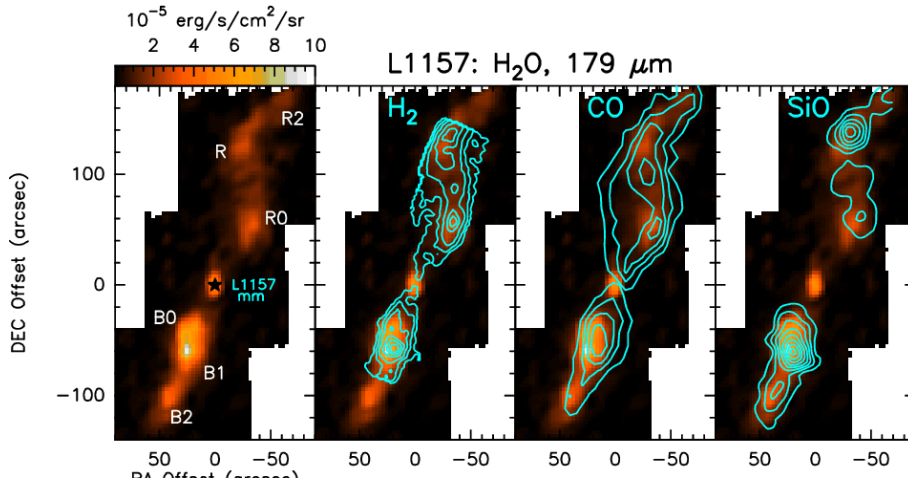
Figure 10: Continuum subtracted PACS map of the integrated H_2O 179 μm emission along the L1157 outflow [29]. The same map is shown in the other panels with overlays of other tracers, namely H_2 0-0 S(1) at 17 μm, CO 2-1, and SiO 3-2.
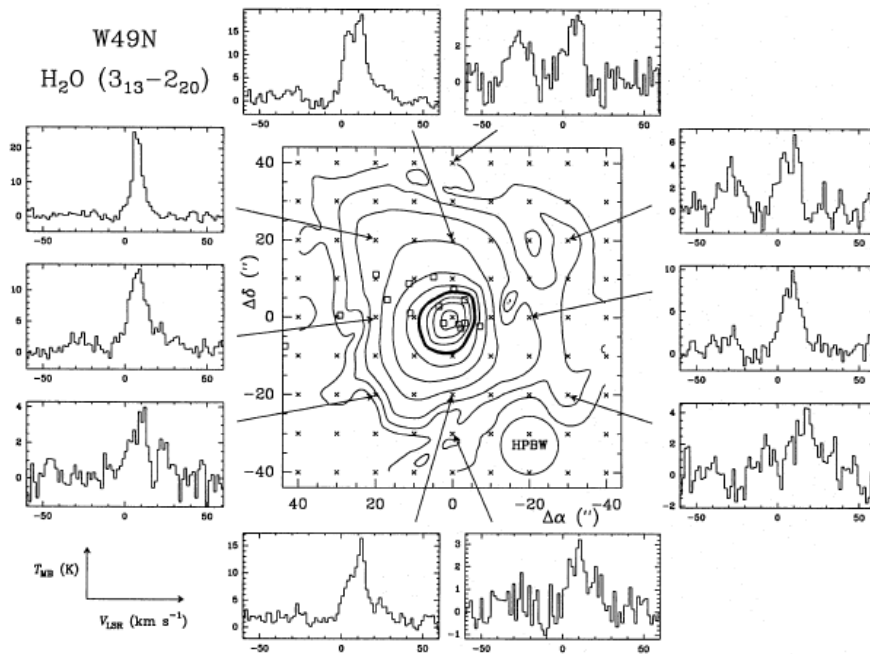

Figure 11: Spatially resolved spectra of 183-GHz water emission from the star-forming region W49N [12].
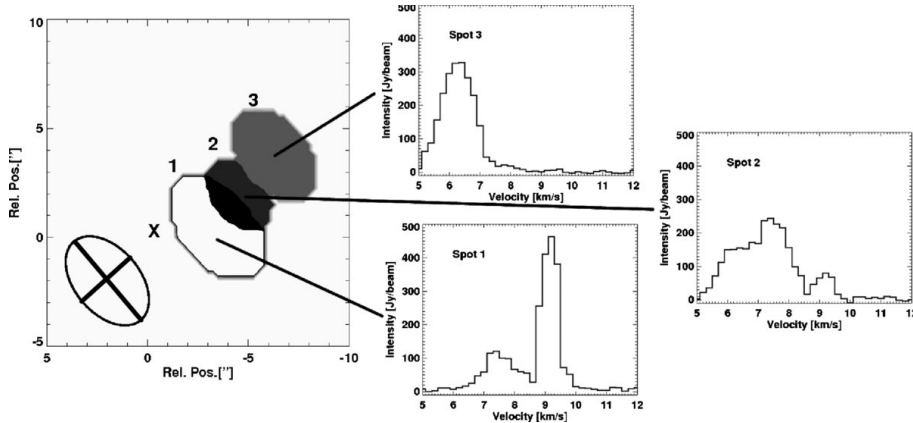
Figure 12: Moment map of the three maser spots in SMM1 [35]. An X marks the maximum intensity of the continuum, which coincides with the location of the protostar. The spectra at the three maser spots are shown.

Persson et al. (in preparation) resolved the emission from this line in the protostellar outflow from NGC 1333 IRAS2A and IRAS4A with the Plateau de Bure interferometer at 203.4 GHz. They suggest that the emission of water in embedded protostars is mostly located in a pseudo-disk produced by the result of infall. In NGC 1333-IRAS4B (Fig. 13; [21]), a velocity gradient is also clearly detected, but it is unclear whether this arises in the hot inner region of the protostellar envelope or the circumstellar disk. Higher-resolution ALMA observations are crucial to an understanding of the complex physics and chemistry in these regions.

4.5   Water masers in circumstellar envelopes

Studies of Asymptotic Giant Branch (AGB) stars are important to our understanding of mass return to the interstellar medium, element enrichment and stellar evolution. A sketch of the principal phenomena in the extended stellar atmosphere is shown in Fig. 14 (left panel). 22 GHz water maser emission has been well-resolved in many evolved stars. It comes from dozens to hundreds of clumps in an approximately spherical shell, extending from roughly 5 to 50 stellar radii. The inner edge is close to the silicate dust formation zone and the wind is gradually accelerated through the escape velocity as it traverses the 22-GHz shell.

Bright 183-GHz maser emission has also been detected in the envelopes of a number of late-type stars [13]. The 22, 183 and 325-GHz maser transitions trace different physical conditions [19]. Fig. 14 (right panel) shows the observed locations of 22 GHz masers round IK Tau, with the putative locations of the higher-frequency transitions overlaid. The 183-GHz emission, which may extend from about 4-18 stellar radii, is of particular interest because it straddles the dust formation zone. The maser kinematics will demonstrate whether that marks the predicted transition between motions dominated by shocks from stellar pulsations (infall as well as outflow) to monotonic expansion. Proper motion studies will also show whether these clouds survive the dust formation process or are re-formed outside 5 stellar radii.

ALMA will measure bright, compact maser spots with precision proportional to (beamsize/snr), giving position accuracies of a few mas even with baselines of a few km (or less, for the brightest emission). This is vital for the required high-resolution kinematic studies and for locating the different species accurately, including with respect to the central star, which ALMA will also detect.

The polarization of the 183-GHz line would also provide an excellent probe of the magnetic-field structure, but measurement would be extremely challenging, as the expected level is only $0.1 - 0.5\%$.

5   Conclusions

We have demonstrated that there is an extremely strong case for a full set of Band 5 ALMA receivers, based primarily on observations of water in the nearby Universe and of redshifted atomic lines at very high redshift. The range and importance of these applications has greatly strengthened over the last few years with the first results from Herschel and the increased emphasis on the Epoch of Reionization in observational cosmology. We therefore believe that Band 5 is a very high priority for the ALMA Development Plan.
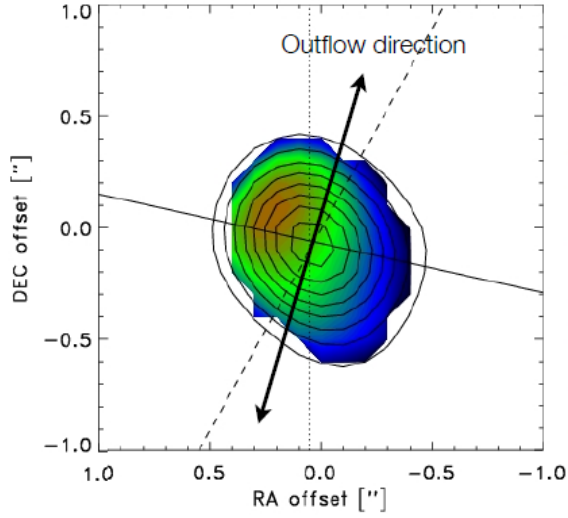
Figure 13: Moment 1 (velocity) map of the $H_2^{18}O$ emission from NGC 1333-IRAS4B, observed with the IRAM PdBI [21].
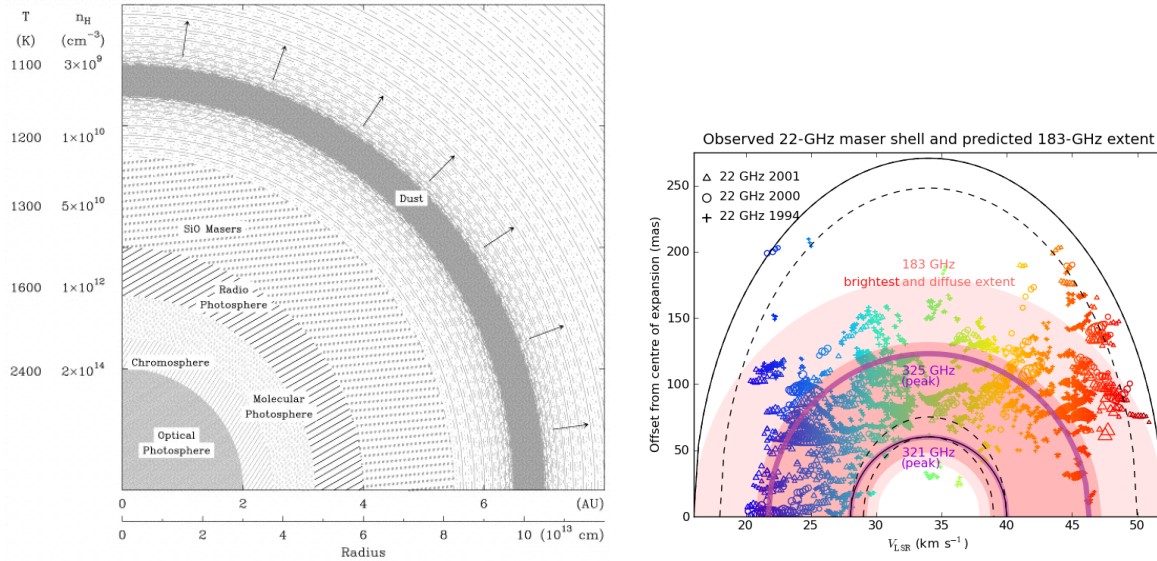

Figure 14: Left: Schematic representation of the radial locations of various phenomena in the extended stellar atmosphere of a long-period variable star [32]. Right: position-velocity plot showing the observed 22-GHz water maser emission from the Oxygen-rich AGB star IK Tau together with the predicted locations of masers at 183, 321 and 325 GHz.

13

Acknowledgements

References

[1] Bergin, E. A., Hogerheijde, M. R., Brinch, C., et al. 2010, A&A, 521, L33

[2] Bergin, E. A., & van Dishoeck, E. F. 2011, arXiv:1110.4152

[3] Bouwens, R. J., Illingworth, G. D., Oesch, P. A., et al. 2010, ApJ, 709, L133

[4] Bouwens, R. J., Illingworth, G. D., Labbe, I., et al. 2011, Nature, 469, 504

[5] Brinch, C., & Hogerheijde, M. R. 2010, A&A, 523, A25

[6] De Breuck, C., Maiolino, R., Caselli, P., et al. 2011, A&A, 530, L8

[7] Cernicharo, J., Gonzalez-Alfonso, E., Alcolea, J., Bachiller, R., & John, D. 1994, ApJ, 432, L59

[8] Cernicharo, J., Bachiller, R., & Gonzalez-Alfonso, E. 1996, A&A, 305, L5

[9] Cernicharo, J., Pardo, J. R., & Weiss, A. 2006, ApJ , 646, L49

[10] Curtis, E. I., Nikolic, B., Richer, J. S., & Pardo, J. R. 2009, ALMA Memo 590 (arXiv:0912.2852)

[11] Encrenaz, T. H., Lellouch, E., Cernicharo, J., et al. 1995, Icarus, 117, 162

[12] Gonzalez-Alfonso, E., Cernicharo, J., Bachiller, R., & Fuente, A. 1995, A&A, 293, L9

[13] Gonzalez-Alfonso, E., Cernicharo, J., Alcolea, J., & Orlandi, M. A. 1998, A&A, 334, 1016

[14] Gurwell, M. A., Bergin, E. A., Melnick, G. J., & Tolls, V. 2005, Icarus, 175, 23

[15] Gurwell, M. A., Melnick, G. J., Tolls, V., Bergin, E. A., & Patten, B. M. 2007, Icarus, 188, 288

[16] Hogerheijde, M. R., Bergin, E. A., Brinch, C., et al. 2011, Science, 334, 338

[17] Hartogh, P., Crovisier, J., de Val-Borro, M., et al. 2010, A&A, 518, L150

[18] Herbst, E., & van Dishoeck, E. F. 2009, ARA&A, 47, 427

[19] Humphreys, E. M. L., Yates, J. A., Gray, M. D., Field, D., & Bowen, G. H. 2001, A&A, 379, 501

[20] Humphreys, E. M. L., Greenhill, L. J., Reid, M. J., et al. 2005, ApJ, 634, L133

[21] Jørgensen, J. K., & van Dishoeck, E. F. 2010, ApJ, 725, L172

[22] Kristensen, L. E., van Dishoeck, E. F., Tafalla, M., et al. 2011, A&A, 531, L1

[23] Maiolino, R., Cox, P., Caselli, P., et al. 2005, A&A, 440, L51

[24] Maiolino, R., Caselli, P., Nagao, T., et al. 2009, A&A, 500, L1

[25] Megamaser Cosmology Project, https://safe.nrao.edu/wiki/bin/view/Main/MegamaserCosmologyProject

[26] Meech et al. 2011, ApJL 734, L1

[27] Miyoshi, M., Moran, J., Herrnstein, J., et al. 1995, Nature, 373, 127

[28] Mortlock, D. J., Warren, S. J., Venemans, B. P., et al. 2011, Nature, 474, 616

[29] Nisini, B., Benedettini, M., Codella, C., et al. 2010, A&A, 518, L120

[30] Pettini, M., Zych, B. J., Steidel, C. C., & Chaffee, F. H. 2008, MNRAS, 385, 2011

[31] Petuchowski, S. J., Bennett, C. L., Haas, M. R., et al. 1994, ApJ, 427, L17

[32] Reid, M. J., & Menten, K. M. 1997, ApJ, 476, 327

[33] Stacey, G. J., Hailey-Dunsheath, S., Ferkinhoff, C., et al. 2010, ApJ, 724, 957

[34] Tanvir, N. R., Fox, D. B., Levan, A. J., et al. 2009, Nature, 461, 1254

[35] van Kempen, T. A., Wilner, D., & Gurwell, M. 2009, ApJ, 706, L22

[36] Walter, F., & Carilli, C. 2008, Ap&SS, 313, 313

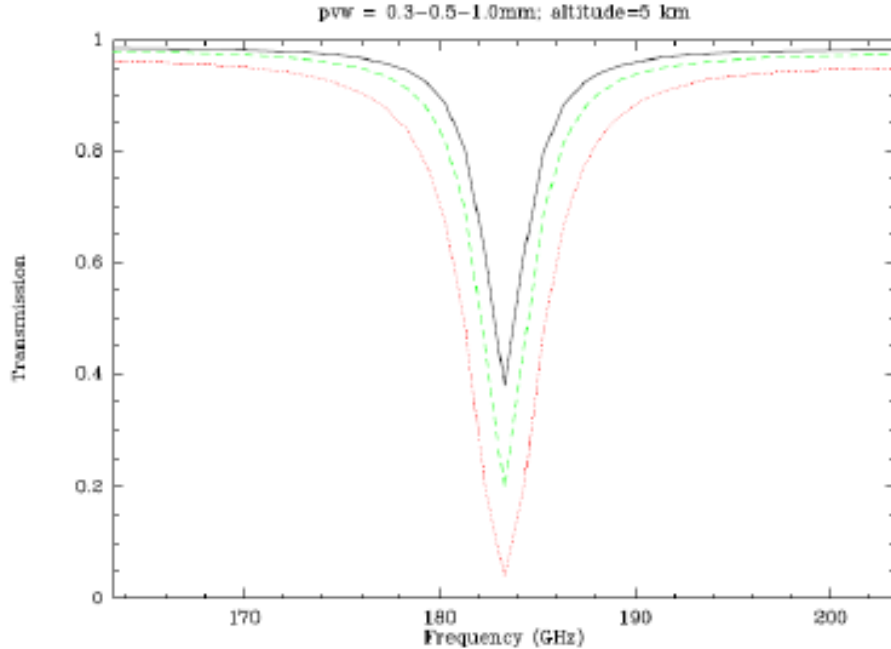[37] Walter, F., Riechers, D., Cox, P., et al. 2009, Nature, 457, 699

Figure 15: Transmission in Band 5 for different columns of precipitable water vapour (PWV).

A   Technical considerations

The atmospheric transmission for different columns of precipitable water vapour is plotted in Fig. 15 and rms continuum noise levels for two representative values of PWV (best and fourth octiles) are given in Table 1. Three of the most important lines for solar system and Galactic observations are H_2O, $H_2^{18}O$ and H_2S. Frequencies and typical noise levels are given in Table 2.

When observing in the vicinity of the atmospheric water line, very careful bandpass calibration will be required. The passband shape is a mix of instrumental bandpass characteristics and the atmospheric water absorption across the band. It is likely that the best approach will be to correct for instrumental terms using a bandpass calibration at the full spectral resolution, but this will almost certainly have to be obtained at a different elevation and under different atmospheric conditions from the target. Additional calibration using spectrally-smoothed data from a nearby source and/or measurements from the water-vapour radiometers will be required. Self-calibration on bright maser sources will also be possible. These approaches are already required for the water lines in Band 7, particularly at 325 GHz. With the exception of WVR correction, they have been demonstrated directly at 183 GHz using SMA data [20, 35].

There is also a significant dispersive term in the path variation across the water line, although this is not as significant as at very high frequencies [10].

Table 1: Representative continuum noise levels in mJy beam^{-1} for three frequencies in Band 5: at the edges of the band and on the water line. An integration time of 1 hour, with 50 antennas is assumed, using a bandwidth of 8 GHz and dual polarization for a source at high elevation.

PWV	ν/GHz		
mm	167	183	211
0.47	0.011	0.083	0.011
1.26	0.012	0.590	0.012

Table 2: Frequencies and noise levels for three of the most important lines in Band 5. An integration time of 1 hour, with 50 antennas is assumed, using a channel width of 1 kms^{-1}. σ is the rms image noise and T is the corresponding rms brightness temperatures assuming a 1 arcsec beam.

Molecule	ν GHz	PWV mm	σ mJy beam^{-1}	T K
H_2O	183.310	0.5	11	0.46
$H_2^{18}O$	203.407	2.3	1.3	0.05
H_2S	168.762	2.3	1.3	0.05